

# 1 Introduction

The increase in global mean surface atmospheric temperature ( $T_A$ ) in recent decades is perhaps the most iconic metric of global warming; the long term trend in  $T_A$  is widely believed to result from the accumulation of energy in the climate as a result of anthropogenic emissions (IPCC). In addition to the multi-decade upward trend,  $T_A$  also exhibits monthly, annual and multi-annual variability where connection between  $T_A$  and global energy content is less clear (*Palmer and McNeall, 2014; Johnson et al., 2009*). Specifically, during the so called global warming hiatus in the first decade of the the 21<sup>st</sup> century,  $T_A$  ceased it's upward trend despite the apparent continued energy accumulation in the climate system (*Medhaug et al., 2017*) – as measured from both satellite radiation and ocean heat content changes (*Loeb et al., 2009*). This suggest that the planet can warm without accumulating energy but, rather, by moving energy from the ocean interior to the surface atmosphere. Here, we explore the mechanisms of sort term global mean temperature variability and argue that:

(1) the dominant mechanism of short term  $T_A$  variability results from the exchange of energy between the ocean and atmosphere as opposed to radiative variability. As a result, short term temperature variability is not accompanied by changes in the energy content of the climate system as a whole.

(2) The exchange of energy between the atmosphere and the ocean is primarily a consequence of surface wind variability which moderates the efficiency of energy exchange between the surface and the atmosphere and requires no changes in atmospheric and or oceanic temperatures. As such, high frequency  $T_A$  variability is *generated by energy fluxes out of the ocean but does not require ocean dynamics*.

The mechanisms that drive the spectrum of surface temperature at regional spatial scales is well understood in the scientific literature. Consider the a simplified bulk parametrization of the upward surface between the ocean/land surface at temperature  $t_S$  and the overlying atmosphere at temperature  $t_A$ :

$$SHF = cU(t_S - t_A), \quad (1)$$

where  $c$  is the transfer coefficient and  $U$  is the surface wind speed (*Fairall et al., 1996*) and lower case  $t$  represent the local temperatures (as opposed to upppercase for global means). Assuming, for now, no variations in  $U$  (we revisit this assumption later) and applying this equation to temperature perturbations from climatology, this equation states that energy will be fluxed away from the fluid with the larger temperature anomaly. As a result, surface atmospheric temperature variability is driven by different mechanisms at high and low frequencies:

**High frequencies** Internal modes of atmospheric dynamics can converge/diverge vast amounts of energy to the regional atmosphere which – because of the relatively small heat capacity of the atmosphere – results in large  $T_A$  variability. In contrast, the large heat capacity of the ocean damps the impact of ocean dynamics om  $T_S$  variability at high frequencies.  $T_A$  variability is driven by atmospheric processes and damped to the ocean (?).  $T_A$  variability is enhanced relative to a fixed SST simulations when the ocean thermodynamically coupled to the atmosphere (i.e. a slab ocean) because there is less damping via the surface heat fluxes when  $T_S$  is allowed to adjust to the surface energy fluxes (*Barsugli and Battisti, 1998*).

**Low frequency** The atmosphere has very little memory in the absence of coupling to the ocean whereas ocean dynamics operate on longer timescales and sustained ocean lateral heat flux convergence and changes in vertical stratification to a region can impact  $T_O$  despite the large ocean

heat capacity. At time scales greater than about 12 years, upward fluxes from the ocean force  $T_A$  variability (*Gulev et al.*, 2013).

The above mechanisms describe regional  $T_A$  but may not apply to the (global)  $T_S$  because they rely on lateral heat flux divergences in the atmosphere and ocean that are large locally, but are – by definition– zero in the global average. Here we present a theoretical framework and present analysis to ask: what processes drive (global)  $T_S$  variability across a hierarchy of different couplings between the atmosphere and ocean ranging from fixed SST to thermodynamic coupling (slab ocean) and to fully coupled (dynamic ocean)?

## 2 Model:

Anomalies in global mean surface atmosphere and sea surface temperature ( $T_A$  and  $T_S$  respectively) are represented by the linearized energy budget of the global atmosphere and ocean:

$$\begin{aligned} C_A \frac{dT_A}{dt} &= -\lambda_{RAD} T_A + SHF \\ C_S \frac{dT_S}{dt} &= F_{RAD} - SHF \end{aligned} \quad (2)$$

where  $C_A$  and  $C_S$  are the heat capacities of the atmospheric column and ocean/land mixed layer,  $\lambda_{RAD}$  is the radiative feedback parameter, SHF is the upward (turbulent plus longwave radiation) energy flux from the surface to the atmosphere and  $F_{RAD}$  is the radiative forcing defined as the radiative anomaly unrelated to the temperature feedbacks which we take to result primarily from shortwave cloud radiative effect. We have made two assumptions in the above formulation: (1) the radiative feedback that represents increased outgoing longwave radiation (OLR) to space as the climate system warms – the combined Planck, water vapor and lapse rate feedbacks– results entirely from atmospheric warming which is justified since less than 15% of OLR emanates from the surface (*Kiehl and Trenberth*, 1997); (2) the radiative forcing goes entirely into the surface which, provided  $F_{RAD}$  is primarily shortwave, is equivalent to assuming no atmospheric shortwave absorption.

We can gain further insight into the forcing and feedbacks on global mean temperature by linearizing the SHF in equation 1 about the anomalies in  $T_A$  and  $T_S$  and surface wind speed ( $U_S$ ):

$$SHF = c\bar{U}(T_A - T_S) + cU'\overline{(T_A - T_O)} \quad (3)$$

where  $c$  is a generalization of the bulk transfer coefficient representing the combined sensitivity of latent and sensible heat fluxes to difference between surface skin temperature and humidity and that of the near surface atmosphere (*Andreas and Murphy*, 1986). Equation 3 states that the anomalies heat flux consists of a thermodynamic term which fluxes energy away from the fluid that has warmed more (with an efficiency that is proportional to the mean surface wind) and a dynamic term where by the climatological air-sea energy exchange is amplified proportional to the anomalous wind stress (with a magnitude that is proportional to the climatological contrast between surface temperature and near surface air temperature). For compactness, we will rewrite equation 2 by defining  $c\bar{U} \equiv \lambda_{SHF}$  akin to the radiative feedback parameter and  $F_{SHF} \equiv cU'\overline{(T_A - T_O)}$  to represent the surface heat fluxes that are unrelated to temperature anomalies and, thus, may force temperature anomalies. Integrating these definitions into the energy budget equations, the evolution of  $T_A$  and  $T_O$  is governed by:

$$\begin{aligned}
C_A \frac{dT_A}{dt} &= -(\lambda_{RAD} + \lambda_{SHF})T_A + \lambda_{SHF}T_S + F_{SHF} \\
C_S \frac{dT_S}{dt} &= -\lambda_{SHF}(T_S - T_A) + F_{RAD} - F_{SHF}
\end{aligned}
\tag{4}$$

In the global mean near surface atmospheric temperature ( $T_A$  evolution equation, the first term acts as a damping term and cannot force variability in  $T_A$  whereas the second and third terms can force  $T_A$ . The value of  $\lambda_{RAD}$  is of order  $2 \text{ W m}^{-2} \text{ K}^{-1}$  (Hansen, 1992) whereas that of  $\lambda_{SHF}$  is an order of magnitude larger which says that, in the absence of concurrent  $T_S$  variability,  $T_A$  will primarily be damped to the ocean. More accurately, the large magnitude of  $\lambda_{SHF}$  is a statement that thermodynamic coupling between the atmosphere and the surface is one of the more efficient (i.e. rapid) processes in the climate system which leads the three generalizable conclusions already touched on in the introduction: (1) dynamic/radiative temperature variability originating from atmospheric processes will be damped to the ocean; (2) the degree of damping will be larger high frequencies and in the fixed SST where the  $T_S$  changes are small/zero and; (3) at low frequencies when internal ocean modes lead to more temperature variability than that in the atmosphere, the atmosphere can be forced by ocean processes. The latter process is encapsulated in the second term ( $\lambda_{SHF}T_S$ ). The last term has received little attention in the literature and results from changes in surface winds moderating the efficiency of air-surface energy exchange in regions of a climatological contrast between the near surface air and surface skin temperature (i.e. in the oceanic western boundary currents). We argue that this forcing term is the dominant mechanism for  $T_A$  variability at time scales less than 3 years in both the fixed SST, thermodynamic and fully coupled climate system.

### 3 Fixed SST simulations.

We first look at CESM1 fixed SST control simulations in a model with full continental geometry, including an interactive land surface with a focus on mechanisms leading to global mean temperature variability. In this setting, variability in the surface radiation ( $F_{RAD}$ ) in the land domain and ocean domains has very different impacts on the overlying atmosphere. Over the land, the surface heat capacity is very small and, as a result, variations in surface radiation heat up the land surface until the upward turbulent fluxes balance the radiative anomaly over a timescale of days. Indeed, at the monthly resolution of the climate model output, SHF is nearly equivalent to  $F_{RAD}$  over the land domain (not shown). In contrast, because ocean temperature are fixed,  $F_{RAD}$  makes no impact on the ocean surface temperature and, thus, this radiative variability over the ocean domain does not result in upward energy fluxes to the atmosphere on any time scale. In the framework of equation 4,  $T_S$  is fixed over the ocean domain and constrained to match that needed to balance  $F_{RAD,LAND}$  over the land domain reducing the  $T_A$  evolution equation to

$$C_A \frac{dT_A}{dt} = -(\lambda_{RAD} + \lambda_{SHF})T_A + F_{RAD,LAND} + F_{SHF}.
\tag{5}$$

Here,  $F_{RAD,LAND}$  is the surface radiative forcing over the land domain associated with shortwave cloud effect but, we note, it could also include the radiative forcing of the atmospheric column which potentially impacts  $T_A$  in the fixed SST setting – we discuss this distinction later in this section. In the fixed SST setting,  $T_A$  is forced by the sum of surface radiative forcing over land ( $F_{RAD,LAND}$ ) and the dynamic component of SHF ( $F_{SHF}$ ) and is by radiative feedbacks ( $\lambda_{RAD}$ ) to

the TOA radiation and thermodynamic coupling to the surface ( $\lambda_{SHF}$ ) via enhanced downward SHF. Since both the radiative fields and SHF that are standard output from climate models will include a combination of the forcing and feedback, the root forcing mechanism for global  $T_A$  variability might not be directly obvious from model output alone.

As a starting point, if we combine the prescribe an external sinusoidal forcing (sum of  $F_{RAD, LAND} + F_{SHF}$ ) with angular frequency  $\omega$  in equation 5 we find that the ratio of the inertial (storage) term to the damping term which much balance the forcing in quadrature phase is :  $\frac{C_A \omega}{\lambda_{RAD} + \lambda_{SHF}}$ . In the limit of high frequency forcing, the forcing is balanced by storage in the column, the temperature will be in quadrature phase and *only the forcing mechanism ( $RAD_{TOA}$  or  $SHF$ ) has appreciable variance at high frequencies since the feedback component of those fluxes is small relative to the forcing*. At low frequencies, the dominant balance is between forcing and feedback and we expect the variance of  $RAD_{TOA}$  and  $SHF$  to be nearly equal in magnitude, contain both forcing and feedback and the  $T_A$  to be nearly in phase with the forcing. The inertial and damping terms are comparable in magnitude when the above ration is unity which corresponds to a forcing period of order 60 days given the atmospheric heat capacity of the atmospheric column ( $10^7 \text{ J m}^{-2}$ ) and typical values of  $\lambda_{RAD}$  ( $2 \text{ W m}^{-2} \text{ K}^{-1}$ ) and  $\lambda_{SHF}$  ( $2 \text{ W m}^{-2} \text{ K}^{-1}$ ) weighted over the fraction of Earth covered by ocean. Thus, we expect an imbalance between the variance in  $RAD_{TOA}$  and  $SHF$  at timescales less than 2 months with the more variance in the forcing mechanism. This expectation is confirmed in Fig. 1A where we see the variance in  $SHF$  exceeds that in  $RAD_{TOA}$  at higher frequencies, suggesting that  $F_{SHF}$  (the dynamical component of  $SHF$ ) exceeds  $F_{RAD}$  and  $T_A$  variability at sub-annual timescales is forced by energy coming out of the ocean despite the absence of SST variability to drive that variability. We consider the implications on the spectra of  $T_A$ ,  $SHF$  and  $RAD_{TOA}$  in the limit of  $T_A$  forced entirely by radiation and  $F_{SHF}$  below.

**Hypothesis I:** Radiative driven temperature variability –  $F_{RAD, LAND} \gg F_{SHF}$

If the dynamic variability of  $SHF$  ( $F_{SHF}$ ) is small, the  $SHF$  can only damp  $T_A$  variability and – since  $\lambda_{SHF} \gg \lambda_{RAD}$  – the radiation at the surface and TOA primarily represent the forcing and the  $SHF$  primarily represent the damping feedback to  $T_A$  variability. As a consequence: *Spectra of energy fluxes:* The  $SHF$  spectra will be red since the  $SHF$  must balance the radiative forcing in the low frequency, damped regime whereas the  $SHF$  variance will decede that of the radiative forcing in the inertial high frequency regime. In contrast, the net radiation will, to first order, be white – matching the stochastic radiative forcing – but slightly blue due to radiative damping (via  $\lambda_{RAD}$  counteracting the forcing at low frequencies).

*Phasing of  $SHF$  and  $T_A$ :* Since the  $SHF$  in this regime is primarily due to damping, energy will be fluxed downward into the surface as the  $T_A$  increases.

**Hypothesis II:** Wind driven temperature variability–  $F_{SHF} \gg F_{RAD, LAND}$

If the variability in the dynamic component of  $SHF$  – induced by wind speed variations – is large compared to the radiative forcing than the  $SHF$  is the combination of the forcing and the damping whereas the radiative fluxes are nearly entirely the damping. **THINK ABOUT MAGNITUDE OF THE  $SHF$**  – at low frequencies forcing and damping nearly in phase so the  $SHF$  variability is reduced due to near cancelation but how big relative to the radiation (damping only)

If the dynamic variability of  $SHF$  ( $F_{SHF}$ ) is small, the  $SHF$  can only damp  $T_A$  variability and – since  $\lambda_{SHF} \gg \lambda_{RAD}$  – the radiation at the surface and TOA primarily represent the forcing and the  $SHF$  primarily represent the damping feedback to  $T_A$  variability. As a consequence: *Spectra of energy fluxes:* The  $SHF$  spectra will be red since the  $SHF$  must balance the radiative forcing in the low frequency, damped regime whereas the  $SHF$  variance will decede that of the radiative forcing

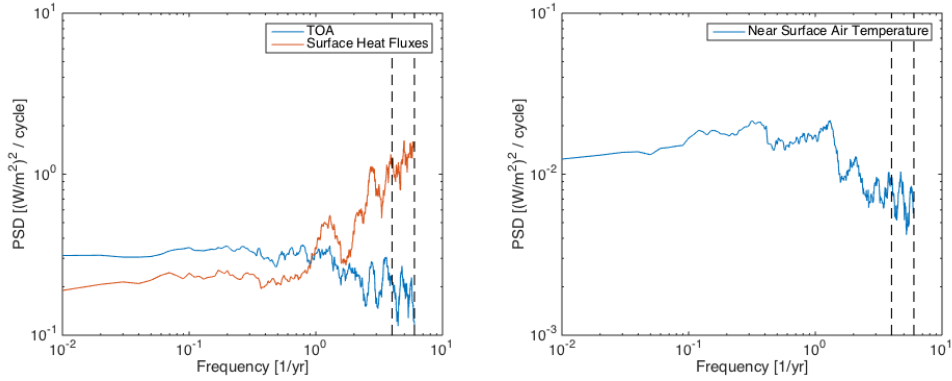


Figure 1: Fixed SST control simulation: Spectra of global mean net surface sensible and latent heat fluxes, TOA radiative imbalance, and surface air temperature

in the inertial high frequency regime. In contrast, the net radiation will, to first order, be white – matching the stochastic radiative forcing – but slightly blue due to radiative damping (via  $\lambda_{RAD}$  counteracting the forcing at low frequencies).

*Phasing of SHF and  $T_A$* : Since the SHF in this regime is primarily due to damping, energy will be fluxed downward into the surface as the  $T_A$  increases.

**Hypothesis II:**  $F_{\mathcal{H},ao} \gg F_{SW,ao}$

The radiative forcing is small, and the system is primarily forced by wind-variance driven stochastic air-sea fluxed,  $F_{\mathcal{H},ao}$ . Consequences:

## 4 Conclusion:

Figure 1 shows that the spectra of global net TOA imbalance and surface heat fluxes are consistent with hypothesis II, wherein the energy in the system is provided by wind variance driven stochastic air-sea fluxes.

## 5 Spatial distribution

The arguments above hold for the global average limit, where the lateral heat flux divergence sums up to zero. The variance of local air-sea fluxes will be higher due to local heat exchanges mediated by lateral transport. However, we can focus on the high-frequency regime highlighted by the dashed-vertical lines in Figure 1, where the atmospheric temperature response is suppressed, to get an intuition for the local source of the forcing. A direct estimate of the forcing component of air-sea fluxes,  $F_{\mathcal{H}}$  could be obtained from the bulk formula by using the 10-m wind variance and climatological specific humidity gradient,  $\Delta q = \overline{q_a} - \overline{q_s}$ . [That has to have been done, right?]

Figure 2 shows the local variance of the net TOA radiative imbalance and the local air-sea fluxes, band passed to  $f \in [4 - 6] \text{ yr}^{-1}$ . The figure would suggest energy extraction over the western part of basins in the mid-latitudes, perhaps consistent with dry air coming from the continents setting up regions of high climatological humidity gradient.

### Fully Coupled Control Run

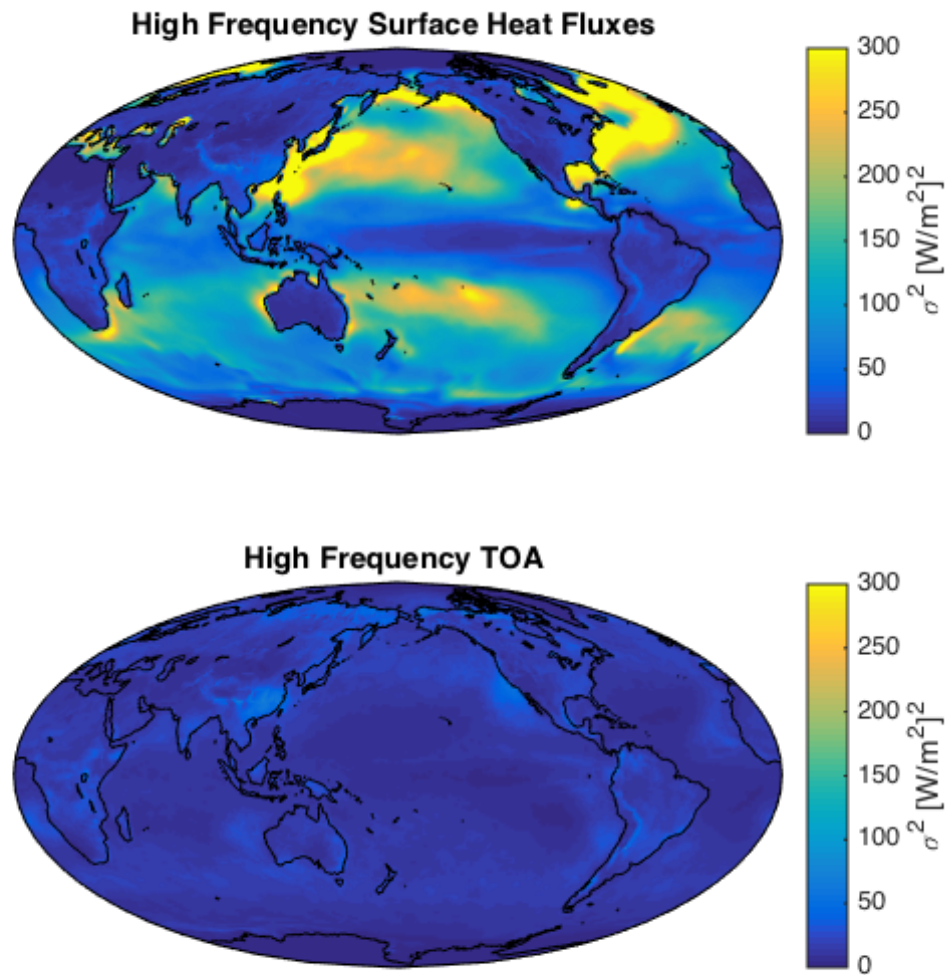


Figure 2: Fixed SST control simulation: Local variance in Net Surface Heat Fluxes and TOA imbalance

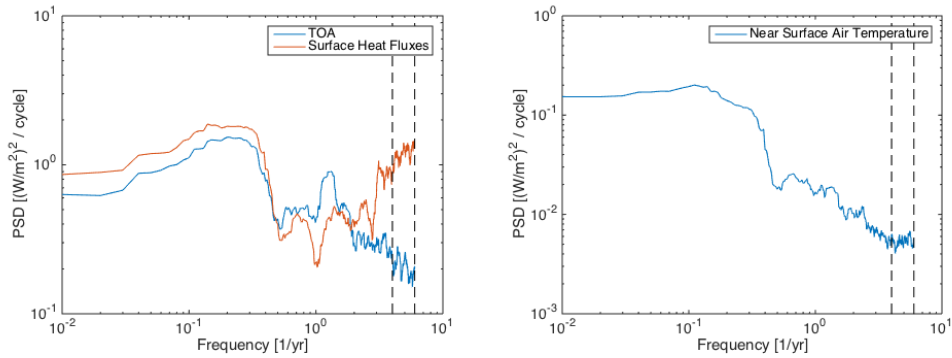


Figure 3: Fully coupled control simulation: Spectra of global mean net surface sensible and latent heat fluxes, toa radiative imbalance, and surface air temperature

Figures 3 & 4 show the spectra and local high-frequency variance fluxes for the fully coupled CESM1 control simulation

## 6 References

### References

- Andreas, E., and B. Murphy (1986), Bulk transfer coefficients for heat and momentum over leads and polynas, *J. Phys. Oceanogr.*, *16*, 1875–1883.
- Barsugli, J., and D. Battisti (1998), The basic effects of atmosphere-ocean thermal coupling on midlatitude variability, *J. Atmos. Sci.*, *55*, 477–493.
- Fairall, C., E. Bradley, D. Rogers, J. Edson, and G. Young (1996), Bulk parameterization of air-sea fluxes for tropical ocean-global atmosphere coupled-ocean atmosphere response experiment, *J. Geophys. Res.*, *101*, 3747–3764.
- Gulev, S., M. Latif, N. Keenlyside, W. Park, and K. Koltermann (2013), North atlantic ocean control on surface heat flux on multidecadal timescales., *Nature*, *494*.
- Hansen, J. e. a. (1992), Efficacy of climate forcings, *J. Geophys. Res.*, *110*(D18), D18,104.
- Johnson, G., J. Lyman, and N. Loeb (2009), Improving estimates of earth’s energy imbalance, *Nat. Clim. Chang.*, *6*(7), 639–640.
- Kiehl, J., and K. E. Trenberth (1997), Earth’s annual global mean energy budget., *Bull. Amer. Meteor. Soc.*, *78*, 197–208.
- Loeb, N. G., B. A. Wielicki, D. R. Doelling, G. L. Smith, D. F. Keyes, S. Kato, N. Manalo-Smith, and T. Wong (2009), Towards optimal closure of the earth’s top-of-atmosphere radiation budget., *J. Climate*, *22*, 748–766.
- Medhaug, I., M. Stolpe, E. Fischer, and R. Knutti (2017), Reconciling controversies about the global warming hiatus, *Nature*, *545*, 41–47.

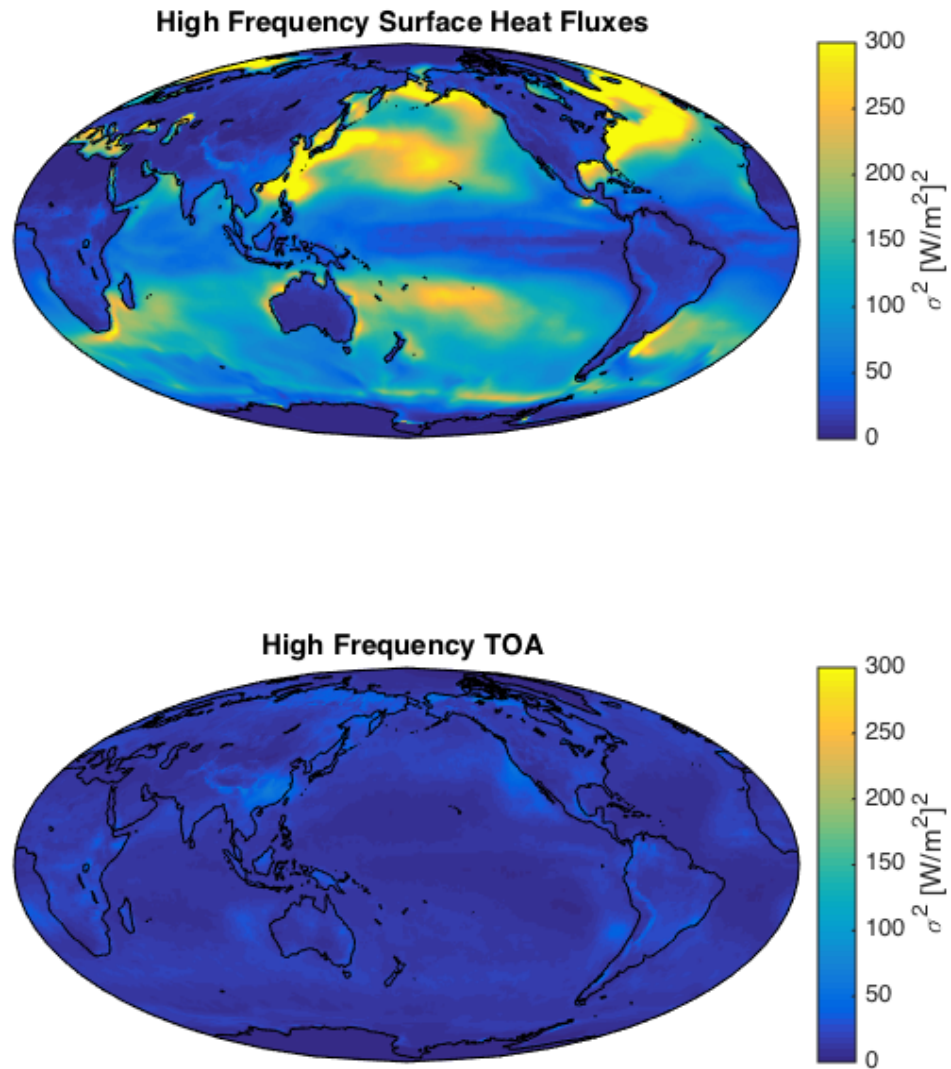


Figure 4: Fully Coupled Control Simulation: Local variance in Net Surface Heat Fluxes and TOA variance

Palmer, M., and D. McNeall (2014), Internal variability of earth's energy budget simulated by cmip5 climate models, *Environ. Res. Lett.*, 9(3), doi:doi:10.1029/2007PA001.